

# Economic-Statistical Design of an Integrated Triple-Component Model Under Various Autocorrelated Processes

Samrad Jafarian-Namin<sup>1</sup>, Mohammad Saber Fallahnezhad<sup>1</sup>, Reza Tavakkoli-Moghaddam<sup>3</sup>, Ali Salmasnia<sup>4</sup> & Mohammad Hossein Abooi<sup>5</sup>

Received 5 June 2020; Revised 12 July 2021; Accepted 2 November 2021;  
© Iran University of Science and Technology 2021

## ABSTRACT

*It has recently been proven that integrating statistical process control (SPC), maintenance policy (MP), and production could bring benefits for the entire production system. In the literature of integrated triple-component models, independent observations have generally been studied. The existence of correlated structures in practice put the traditional control charts in trouble. The mixed EWMA-CUSUM (MEC) chart has been developed as an effective tool of SPC for monitoring only the autoregressive (AR) processes. Nevertheless, it has not been extended for moving average (MA) and ARMA processes. Besides, MEC has been designed only based on statistical measures. However, in an imperfect production system, the decision variables of MEC together with the other components should be determined according to the resulting costs and satisfaction of some criteria. This paper proposes an integrated triple-component model by applying the MEC chart for monitoring various autocorrelated processes. Due to the complexity of the model, a particle swarm optimization (PSO) algorithm is employed to reach optimal solutions. The applicability of the model is investigated via an industrial example. The effects of model parameters on the solutions are studied through a sensitivity analysis. Moreover, extensive comparisons and a real data set are provided for more investigations.*

**KEYWORDS:** *Statistical process control; Production; Maintenance policy; Autocorrelated process; Meta-heuristic algorithm.*

## 1. Introduction

In today's world of competition, it is essential to provide appropriate planning for manufacturing systems to survive. The component of the economic production quantity (EPQ) has classically been pursued by minimizing the production and inventory costs to respond to the demand of a customer [1]. In such perfect production systems that only consider EPQ, the process is basically faultless. Due to various reasons, the process perhaps deteriorates over

time in reality. The related costs and losses are ignored in the category of perfect production. The statistical process control (SPC) and maintenance policy (MP) are commonly used to raise the quality and efficiency of production systems by decreasing the proportion of non-conforming products. Simultaneous consideration of EPQ, SPC, and MP forms the category of imperfect production systems.

Separately modeling of triple components, including EPQ, SPC, and MP, leads to suboptimal results because of their interaction [2-4]. Detecting such dependency can reduce the operational cost and improve the efficiency of manufacturing systems. Hadidi et al. [5] reviewed the researches of such models in two directions: (1) interrelated models, in which one component is considered as the objective and the others are taken into account as constraints, and (2) integrated models, in which two or more components are simultaneously considered as the objective and some required constraints are defined. The relationships among the triple

\* Corresponding author: *Mohammad Saber Fallahnezhad*  
[fallahnezhad@yazd.ac.ir](mailto:fallahnezhad@yazd.ac.ir)

1. Department of Industrial Engineering, Faculty of Engineering, Yazd University.
2. Department of Industrial Engineering, Faculty of Engineering, Yazd University.
3. School of Industrial Engineering, College of Engineering, University of Tehran.
4. Department of Industrial Engineering, Faculty of Technology and Engineering, University of Qom.
5. Department of Industrial Engineering, Faculty of Engineering, Yazd University.

components have motivated scholars to study the integrated models more than before. Recently, Farahani and Tohidi [6] reviewed the literature on integrated optimization. Their results indicate that 63% of the researches are related to the integration of SPC and MP, and 31% is related to the integration of triple components. The current study also considers the integrated triple-component models that need more attention.

Among those components, SPC aims to improve quality through variability reduction. The control chart is among the seven tools of SPC. It is mainly applied to identify the variations of the process before producing defective items in higher volumes. Numerous control charts have been developed for monitoring processes under various assumptions to attain specific intentions [7]. The independence of the sampled data over time is usually assumed. Among recent studies under this assumption, the designs of the acceptance control chart (ACC) were presented with Duncan's cost function [8] and with Lorenzen and Vance's (L&V) cost function [9]. The reader can see [10] for integrating the EPQ and SPC, [11] for integrating SPC and MP, and [3, 4] for the integrated triple-component models under the assumption of independence.

However, the independence assumption can be violated when: (1) autocorrelation is induced by sampling in high frequency from some processes, and (2) it inherently exists among the process data [12]. The ignored autocorrelation can lead to significant effects on the statistical performance of traditional monitoring techniques [13]. Indeed, it leads to numerous false alarms in the in-control state or makes the classical control charts react slowly to detecting out-of-control state. Several control charts have been extended for this reason under two main approaches, including the residual control charts and the modified control charts [14]. The main advantages of modified control charts include: (1) directly monitoring the autocorrelated data and (2) more straightforward interpretation by the operator. Accordingly, modified control charts are selected for monitoring in this study.

Among the modified charts, the mixed EWMA-CUSUM chart (MEC) was developed in [15] for monitoring only AR(1) process data under various sizes of mean shifts. For positively autocorrelated processes with smaller mean shifts, the results indicated that MEC was slightly better than the other existing modified charts such as the Shewhart, CUSUM, EWMA, combined Shewhart-CUSUM, and combined Shewhart-EWMA schemes. However, MEC has

not been extended for ARMA and MA processes. Moreover, its design and performance have been investigated only based on statistical criteria. Whereas in an imperfect production system, determining the decision variables of MEC needs attention to other components and the resulting costs.

On the other hand, the ARMA control chart is an appropriate monitoring technique for ARMA(1,1) and AR(1) processes [16]. It benefits from allowing a more flexible choice of parameters for the underlying process. The statistical performance of the ARMA chart is superior to the performance of the SCC and EWMAST charts [16]. The design of the ARMA chart has been studied by a few researchers. Economical designs (ED) of the ARMA chart for optimal selection of decision variables were presented in [17, 18] by respectively minimizing the Duncan's and L&V's cost functions. Because of the poor statistical properties of EDs, the decision variables of the ARMA chart were optimally determined through the economic-statistical design (ESD) based on L&V's cost function [19, 20]. After reviewing the literature in [21, 22], it was concluded that autocorrelation was not incorporated into the integrated models. For the first time, integrated models of double and triple components with three scenarios [21] and ten scenarios [22] were recently studied by considering autocorrelation. They applied the ARMA control chart for monitoring. Their results indicated that integrated triple-component models were superior to double-component ones in terms of total cost reduction. Accordingly, this study also considers a model by integrating triple components.

Despite successful applications of MEC and ARMA charts compared to the other ones, there is not any research to suggest which one is superior. It needs more investigations to realize a better monitoring technique. Attempting in this regard can be more realistic in the framework of imperfect production systems, especially when optimizing an integrated model of triple components is considered. To the best of our knowledge, MEC has not been applied to (1) the other autocorrelated processes, such as ARMA(1,1) and MA(1), and (2) the integrated models under autocorrelated processes. Accordingly, this study aims at bridging the existing gaps in the literature by:

- Applying MEC chart for an imperfect production system under autocorrelated processes,
- Finding the significant factors that affect

on the optimal results,

- Comparing the results of MEC and ARMA charts for the proposed model,
- Investigating various autocorrelated processes, and,
- Using different designs of setting decision variables in a real application.

The rest of this paper is organized as follows. In the next section, various autocorrelated structures are briefly described. Section 3 is dedicated to the introduction of the MEC and ARMA charts as well as proposing procedures for calculating the performance measures. Section 4 presents an imperfect production process, including three scenarios together with its cost function of triple components. Section 5 proposes the integrated model in detail. Section 6 proposes and explains the solution approach based on PSO. Section 7 provides the experimental results, including industrial examples, sensitivity analysis, and extensive comparisons. Finally, Section 8 provides a conclusion and further perspectives.

### 2. Autocorrelated Structures

Supposing that the measured quality variable at time  $t$ , indicated by  $X_t$ , follows a Normal distribution with in-control mean  $\mu_0$  and variance  $\sigma^2$ , the first-order autoregressive moving average process or ARMA(1,1) is mathematically expressed by:

$$X_t = C + uX_{t-1} + a_t - va_{t-1}, \quad a_t \in N(0, \sigma_a^2), \quad (1)$$

where  $C = \mu_0(1-u)$  is a constant term, and  $u$  and  $v$  are the autoregressive and moving average coefficients with conditions  $|u| < 1$  and  $|v| < 1$ , respectively. Moreover, the sequence of random variables  $a_t, a_{t-1}, a_{t-2}, \dots$  is called the white noise process. If  $v=0$ , a particular type of ARMA(1,1) process, called the first-order autoregressive process or AR(1) is achieved as follows:

$$X_t = C + uX_{t-1} + a_t. \quad (2)$$

Another particular type of ARMA(1,1) process, called the first-order moving average process or MA(1) is attained by setting  $u=0$  as follows:

$$X_t = C + a_t - va_{t-1}. \quad (3)$$

The variance of the ARMA(1,1) process is calculated by:

$$Var(X_t) = \sigma_X^2 = \frac{1-2uv+v^2}{1-u^2} \sigma_a^2, \quad (4)$$

Note that the variances of AR(1) and MA(1) processes can be obtained by setting  $u=0$  and  $v=0$  in the above formula, respectively.

By applying a special cause, a positive shift size of  $\delta\sigma_X$  is introduced into the autocorrelated process. It leads to a shift in the in-control mean. The shifted observations ( $W_t$ ) originated from the shifted ARMA process are obtained by:

$$W_t = X_t + \delta\sigma_X = uX_{t-1} + a_t - va_{t-1} + \delta\sigma_X \quad (5)$$

with the following characteristics:

$$E(W_t) = \mu_1 = \mu_0 + \delta\sigma_X, \quad (6)$$

$$Var(W_t) = \sigma_W^2 = \sigma_X^2 = \frac{1-2uv+v^2}{1-u^2} \sigma_a^2. \quad (7)$$

### 3. Control Charts

In this section, two monitoring techniques are introduced from the category of modified control chart. Both MEC and ARMA charts monitor the observations instead of residuals. Moreover, two procedures are proposed to calculate the in-control and out-of-control performance measures through simulations.

#### 3.1. MEC chart

The MEC chart was modified by [15] for autocorrelated observations. The effectiveness of the MEC control chart has been proven for monitoring AR(1) process. However, investigating its performance for other types of autocorrelated data has remained without any extensions. In this study, ARMA(1,1) and MA(1) processes are investigated by the MEC control chart in addition to the AR(1) process. This chart utilizes two statistics for monitoring the process data as shown below:

$$MEC_t^+ = \max(0, Z_t - \mu - K + MEC_{t-1}^+), \quad (8)$$

$$MEC_t^- = \max(0, -Z_t + \mu - K + MEC_{t-1}^-), \quad (9)$$

where the reference value and decision interval value are defined by  $K = k_c \sigma_z$  and  $H = h_c \sigma_z$ , respectively.  $k_c$  and  $h_c$  are related coefficients that are sought as decision variables in this study. The values of positive and negative  $MEC_t$  are initially set to zero. Moreover, the EWMA statistic  $Z_t$  and its asymptotic variance are respectively defined by:

$$Z_t = \lambda_c W_t + (1 - \lambda_c) Z_{t-1}, \quad (10)$$

$$\sigma_Z^2 \approx \sigma_X^2 \left( \frac{\lambda_c}{2 - \lambda_c} \right) \left\{ 1 + 2 \sum_{i=1}^m \rho_i (1 - \lambda_c)^i [1 - (1 - \lambda_c)^{2(m-i)}] \right\}, \quad (11)$$

where  $\lambda_c$  is the smoothing parameter, and  $\rho_i$  is the autocorrelation function  $X_t$  at lag  $i$ .  $m$  is an integer value. It is suggested to be 25 in general [23]. This chart signals an out-of-control state if at least one of the MEC statistics exceeds the decision interval value:

$$MEC_t^+ > H \quad \text{or} \quad MEC_t^- > H \quad (12)$$

For obtaining average run length (ARL) values, the ARMA simulation (AS) procedure is proposed for the MEC chart in the following steps (note that the procedure is adapted to AR(1) process by setting  $v=0$ ):

**Step 0.** Consider pre-assumed values of  $\mu_0$ ,  $\sigma_X^2$ ,  $u$ , and  $v$ , and then calculate  $\sigma_a^2$ .

**Step 1.** In each column of  $j=1, \dots, S$  scenarios, generate series  $a_{i,j}$ ,  $X_{i,j}$ ,  $W_{i,j}$ , and  $Z_{i,j}$  for  $i=1, \dots, M$  measurements.

**Step 2.** Set related decision variables (i.e., sample size ( $n$ ), sampling interval ( $h$ ),  $h_c$ ,  $k_c$ , and  $\lambda_c$ ).

**Step 3.** Calculate  $\sigma_Z^2$ , the reference value  $K=k_c\sigma_Z$  and the decision interval value  $H=h_c\sigma_Z$ .

**Step 4.** Compute  $RL$  values for  $j=1, \dots, S$ :

- Compute  $RL_{0j}$  until  $MEC_t^+ > H$  or  $MEC_t^- > H$ , by obtaining MEC statistics based on  $X_{i,j}$ ,
- Compute  $RL_{1j}$  until  $MEC_t^+ > H$  or  $MEC_t^- > H$ , by obtaining MEC statistics based on  $W_{i,j}$ .

**Step 5.** Calculate  $ARL_0$  and  $ARL_1$  by averaging them for  $S=500$  times from Step 4.

### 3.2. ARMA chart

The ARMA chart was developed in [16]. The sample statistic to be monitored by this chart at time  $t$  is represented by:

$$Z_t = \phi Z_{t-1} + \theta_0 X_t - \theta X_{t-1}, \quad \beta = \theta/\theta_0, \theta_0 = 1 + \theta - \phi \quad (13)$$

where  $\phi$  and  $\theta$  are the autoregressive and the moving average parameters, respectively. Note that the conditions  $|\phi| < 1$  and  $|\theta| < 1$  must be satisfied to guarantee reversibility and stationary of the process being monitored. The mean of the sample statistic is  $\mu$ , and the corresponding steady-state variance is as follows:

$$\sigma_Z^2 = \left[ \frac{2(\theta - \phi)(1 + \theta)}{1 + \phi} + 1 \right] \sigma_X^2. \quad (14)$$

The upper and lower control limits are calculated by ( $l$  is the control limit coefficient):

$$[LCL, UCL] = [\mu \pm l \sigma_Z]. \quad (15)$$

The AS procedure introduced in the previous subsection is adapted to the ARMA chart to calculate ARL values. The steps of the procedure are summarized as follows:

**Step 0.** Consider pre-assumed values of  $\mu_0$ ,  $\sigma_X^2$ ,  $u$ , and  $v$ , and then calculate  $\sigma_a^2$ .

**Step 1.** In each column of  $j=1, \dots, S$ , generate series  $a_{i,j}$ ,  $X_{i,j}$  and  $W_{i,j}$  for  $i=1, \dots, M$  measurements.

**Step 2.** Set related decision variables:  $n$ ,  $h$ ,  $l$ ,  $\phi$ ,  $\theta$ .

**Step 3.** Obtain the value of steady-state variance  $\sigma_Z^2$ , and the control limits  $UCL$  and  $LCL$ .

**Step 4.** Compute  $RL$  values for  $j=1, \dots, S$ :

- Compute  $RL_{0j}$  until  $LCL \leq Z_{i,j} \leq UCL$ , by obtaining  $Z_{i,j}$  based on  $X_{i,j}$ ,
- Compute  $RL_{1j}$  until  $LCL \leq Z_{i,j} \leq UCL$ , by obtaining  $Z_{i,j}$  based on  $W_{i,j}$ .

**Step 5.** Calculate  $ARL_0$  and  $ARL_1$  by averaging them for  $S=500$  times from Step 4.

## 4. Integrated Cost Function

In this section, an imperfect production process of triple components is introduced. It operates in the in-control or out-of-control states. The related cost function is explained according to the problem at hand. Accordingly, the main assumptions are introduced in the first subsection. Then, three scenarios to include different states of the process are defined. Finally, the structure of the cost function is described.

### 4.1. Assumptions

The considered assumptions for simplifying mathematical modeling are listed as follows:

1. The measured variable follows a normal distribution  $N(\mu, \sigma)$ .
2. The autocorrelation structure among data is of the types AR(1), MA(1), and ARMA(1,1).
3. The cycle always starts from the in-control state.
4. The in-control time of process follows a truncated Weibull distribution (with scale parameter  $\lambda > 0$  and shape parameter  $w > 0$  as):

$$f(t | (k+1)h) = \frac{\lambda w (\lambda t)^{w-1} e^{-(\lambda t)^w}}{1 - e^{-(\lambda(k+1)h)^w}}, \quad (16)$$

5. Occurring a special cause changes the process state to the out-of-control as  $\mu_1 =$

$\mu_0 + \delta\sigma$ .

6. Two types of maintenance policies can be performed according to the following conditions:
  - a. If after the  $k$ -th sampling interval no signal is detected due to falling a point outside the control limits, preventive maintenance (PM) is implemented at the end of the interval  $(k+1)$ ,
  - b. If the process shifts to the out-of-control state in the sampling interval between  $(0 < i < k)$ , the search for the assignable cause begins. Then, reactive maintenance (RM) is implemented to restore the process to the initial condition,
7. Whenever RM is performed after a true signal from the control chart or sampling  $(k+1)$  is implemented (each one occurs earlier), the production cycle is completed.

### 4.2. Scenario description

The production process starts from the in-control state, and due to an assignable cause, it shifts to the out-of-control (Ooc) state after a while. Three possible scenarios, as indicated by  $Sc_r$ ,  $r=1,2,3$  in Figure 1, may occur in an imperfect production process [3].

$Sc_1$  occurs when the process remains in control until the end of the cycle. Then, PM is

implemented to ensure the reliability of the production process. If the process shifts to an out-of-control state, and then this deviation is identified before the end of the cycle,  $Sc_2$  occurs. Therefore, RM is implemented to restore the process state to the initial condition. In  $Sc_3$ , the process shifts to an out-of-control state as well. However, the control chart cannot identify the shift until the end of the cycle. At this time, the shift is detected, and thus, PM is replaced by RM. The probability of occurrence for each scenario  $Pr(Sc_r)$  as well as the expected values of in-control time  $E(T_{in})$  and out-of-control time  $E(T_{out})$  are presented in Table 1. The notations are as follows:

- $F(.)$  : cumulative function of the truncated Weibull distribution,
- $P(\text{signaling} | \text{Ooc state})$  : probability of triggering an alarm when the process shifts to the Ooc state,
- $E$  : time to sample and chart one item,
- $T_1$  : time to detect the assignable cause, and
- $\tau$  : expected time between the assignable cause occurrence and the next inspection.

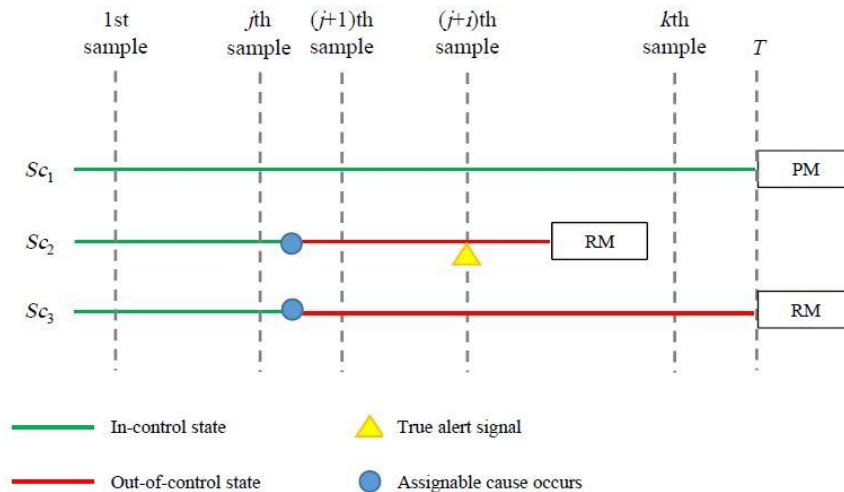


Fig. 1. Graphical representation of scenarios

Tab. 1. Probability and expected time values of occurring each scenario

$r$	$Pr(Sc_r)$	$E(T_{in} Sc_r)$	$E(T_{out} Sc_r)$
1	$1 - F((k+1)h) = e^{-(\lambda(k+1)h)^y}$	$(k+1)h$	0
2	$F(kh)P(\text{signaling}   \text{Ooc state})$	$\int_0^{kh} t \times f(t   (k+1)h) dt$	$h \times ARL_1 - \tau + nE + T_1$
3	$F((k+1)h) - F(kh)P(\text{signaling}   \text{Ooc state})$	$\int_0^{(k+1)h} t \times f(t   (k+1)h) dt$	$(k+1)h - E(T_{in}   Sc_3)$

### 4.3. Structure of cost function

The expected total cost is presented as follows:

$$ETC_{QIM} = E(Q) + E(S) + E(M) + E(I). \quad (17)$$

where it includes the quality loss cost  $E(Q)$ , sampling cost  $E(S)$ , maintenance cost  $E(M)$ , and inventory-related costs  $E(I)$ . Before describing the mentioned items, it is necessary to define the following notations:

- $Q_{in}$  : quality loss cost in the in-control state,  
 $Q_{out}$  : quality loss cost in the out-of-control state,  
 $p$  : production rate,  
 $C_f$  : fixed cost of sampling,  
 $C_v$  : variable cost of sampling,  
 $C_y$  : false alarm cost,  
 $C_{pm}$  : preventive maintenance cost,  
 $C_{rm}$  : reactive maintenance cost,  
 $s$  : expected number of samples when the process is in the in-control state,  
 $B$  : inventory holding cost per unit time,  
 $d$  : daily demand,  
 $A$  : ordering cost, and  
 $E(T)$  : process cycle time.

The detailed information about the constituents of  $ETC$  are described as follows [21]:

1. The quality loss cost is expressed as:
- 2.

$$E(Q) = \sum_{r=1}^3 E(C_Q | Sc_r) \Pr(Sc_r), \quad (18)$$

with expected quality loss cost for each scenario as:

$$E(C_Q | Sc_r) = \begin{cases} Q_{in} \times p \times E(T_{in} | Sc_r), & r=1 \\ Q_{in} \times p \times E(T_{in} | Sc_r) + Q_{out} \times p \times E(T_{out} | Sc_r), & r=2,3 \end{cases} \quad (19)$$

3. The sampling cost per cycle time is formulated as:

$$E(S) = \sum_{r=1}^3 E(C_S | Sc_r) \Pr(Sc_r), \quad (20)$$

with expected sampling cost per cycle time for each scenario as:

$$E(C_S | Sc_r) = \begin{cases} (C_f + C_v n) k, & r=1,3 \\ (C_f + C_v n)(E(T_{in} | Sc_r) + E(T_{out} | Sc_r)) / h, & r=2 \end{cases} \quad (21)$$

4. The maintenance cost per production cycle is computed as:

$$E(M) = \sum_{r=1}^3 E(C_M | Sc_r) \Pr(Sc_r), \quad (22)$$

with expected maintenance cost per production for each scenario as:

$$E(C_M | Sc_r) = \begin{cases} \frac{k \times C_y}{ARL_0} + C_{pm}, & r=1 \\ \frac{s \times C_y}{ARL_0} + C_{rm}, & r=2,3 \end{cases} \quad (23)$$

5. The inventory holding and ordering costs are respectively formulated as:

$$IHC = \frac{B \times E(T) \times (p - d)}{2}, \quad (24)$$

$$OC = \frac{D \times A}{p \times E(T)}. \quad (25)$$

According to the total cost function, the mathematical model is presented in the next section. Moreover, the economic production quantity can be computed by:

$$Q = p \times E(T). \quad (26)$$

## 5. Proposed Model

This section explains the proposed mathematical model according to the defined problem. It includes an objective function based on the expected total cost subject to some constraints as follows:

Min  $ETC_{QIM}$

s.t.

$$\begin{aligned} ARL_0 &\geq ARL_0^{min} \\ ARL_1 &\leq ARL_1^{max} \\ kh &\geq R_{int} \\ nE &\leq h \\ n_{min} &\leq n \leq n_{max}, \quad h_{min} \leq h \leq h_{max} \\ h_{cmin} &\leq h_c \leq h_{cmax}, \quad k_{min} \leq k \leq k_{max} \\ k_{cmin} &\leq k_c \leq k_{cmax}, \quad \lambda_{cmin} \leq \lambda_c \leq \lambda_{cmax} \end{aligned} \quad (27)$$

where the first and the second constraints maintain reasonable  $ARL_0$  and  $ARL_1$  values. The continuity of the process is ensured by the third constraint. Moreover, the fourth one guarantees the solutions that their time of taking and charting samples is lower than the sampling interval ( $h$ ). Besides, the decision variables are set between the limits that may be determined according to the process requirements or suggested by the decision-maker (DM), who has expertise in quality engineering and process control.

Recently, a similar model has been validated for autocorrelated processes [21]. We altered the model by considering the MEC control chart. Six decision variables, including  $n$ ,  $h$ ,  $h_c$ ,  $k$ ,  $k_c$ , and  $\lambda_c$ ,

are determined through optimizing the proposed model. We also use the ARMA chart. For this reason, the constraints of  $h_c$ ,  $k_c$ , and  $\lambda_c$  are respectively replaced by  $l_{min} \leq l \leq l_{max}$ ,  $\theta_{min} \leq \theta \leq \theta_{max}$ , and  $\phi_{min} \leq \phi \leq \phi_{max}$  in the model. In the next section, an approach to optimize the proposed model is provided.

### 6. Solution Approach

It is needed to solve nonlinear programming (NLP) together with some constraints. The decision variables  $h_c$ ,  $\lambda_c$ , and  $k_c$  for the MEC chart and  $l$ ,  $\theta$ , and  $\phi$  for the ARMA chart are merely applied to obtain *ARL* values. Thus, *ETC* is indirectly affected by those variables. On the other hand, the simultaneous presence of both continuous and discrete decision variables leads to the non-convex solution space. Accordingly, exact methods cannot be suitable since the model is not solvable or needs much more time to run. Using metaheuristic algorithms is suggested under such conditions to attain near-optimal solutions in a reasonable time (refer to [8], [21, 22], and [24]).

Of those, PSO, as a stochastic population-based algorithm with powerful searching capacity by combining local and global searches, is chosen to optimize the model. The computational efficiency and easy execution are the other advantages for its wide applications [25]. It has been suitably applied in discontinuous space for solving NLP models [3, 4]. There exist three constraints in the proposed model. Using PSO needs to convert the model into an unconstrained one. Accordingly, a penalized objective function (*fp*) is defined to add any violations from the constraints for pushing back the solution to the feasible region:

$$fp = ETC_{QIM} \times (1 + viol_1 + viol_2 + viol_3), \quad (28)$$

where  $viol_1 = \max(0, 1 - (ARL_0 / ARL_0^{\min}))$ ,  $viol_2 = \max(0, 1 - (kh / R_{int}))$ , and  $viol_3 = \max(0, (nE/h) - 1)$  are the violations from the corresponding constraints. Figure 2 shows the flowchart of the optimization procedure. According to the calibrating results for optimizing a similar model in [21], we set the PSO parameters by considering inertia weight  $w=1.2$ , recognition, and social learning factors  $c_1=c_2=2$ , population size  $N=80$ , and iteration

number  $m=150$ . The steps of the PSO algorithm to optimize the proposed model are employed as follows:

**Step 1. Initialization.** Set the bounds in the model according to DM's considerations and the PSO parameters. Each solution (particle) is shown by position  $X_i^t = [n, h, h_c, k, \lambda_c, k_c]$  and velocity  $V_i^t$  in the iteration  $t$  (note that discrete variables including  $n$ , and  $k$  are transformed to continuous ones). Then, for each particle  $i=1, \dots, N$ :

- Based on Uniform distribution, generate the initial value of position for each particle using a random vector  $X_i \sim U(b_l, b_u)$  and the initial value of velocity according to  $V_i \sim U(-|b_u - b_l|, |b_u - b_l|)$ , where  $b_l$  and  $b_u$  are indications of lower and upper limits of the search space, respectively.
- Initialize the *pbest* of each particle equal to its initial position as  $pbest_i \rightarrow X_i$  (note that *pbest*, called personal best, is the best value experienced by the  $i^{th}$  particle).
- If  $fp(pbest_i) \leq fp(gbest)$ , update  $gbest \rightarrow pbest_i$  (the best solution found so far, called global best, is indicated by *gbest*).

**Step 2. Repetition.** Since the behavior of any particle is affected by the current velocity, the personal best, and the global best, it is necessary to update the velocity and the position in each iteration. In other words, for each particle  $i=1, \dots, N$  and the dimension of each particle  $di=1, \dots, n_{di}$ :

- Generate random numbers  $r_p$  and  $r_g$  from  $U(b_l, b_u)$ .
- Update the particle velocity by  $V_i^t = wV_i^{t-1} + c_1r_p(pb_{est_i}^{t-1} - x_i^{t-1}) + c_2r_g(gbest_i^{t-1} - x_i^{t-1})$ ,
- Update the particle position by  $x_i^t = x_i^{t-1} + V_i^t$ ,
- If  $fp(x_i) \leq fp(pbest_i)$ , update *pbest* of each particle,
- If  $fp(pbest_i) \leq fp(gbest)$ , update *gbest*.

**Step 3. Stopping.** If a predetermined number of iterations is achieved, stop. The latest *gbest* holds the best solution achieved. Otherwise, go back to Step 2.

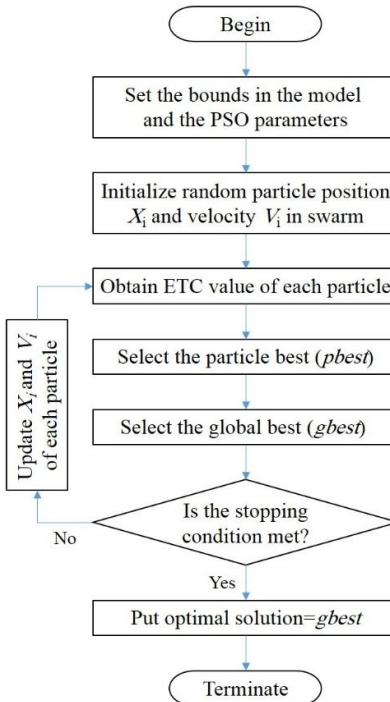


Fig. 2. Procedure of the PSO algorithm

## 7. Experimental Results

For achieving the optimal decision variables related to the production cycle, the cost function of the proposed model needs to be minimized, subject to some constraints. In this regard, an industrial example is extended for the problem at hand to indicate the model's applicability using both monitoring techniques. Then, a comprehensive sensitivity analysis to study the effect of model parameters on the solutions is implemented by considering the MEC chart (similar analysis can be found in [21] using the ARMA chart). Next, some comparisons are made in detail between those monitoring techniques. Finally, a real data set is provided for investigating the issue of separately setting some decision variables against the simultaneous determination of those variables.

### 7.1. Numerical example

For illustrating the determination of decision variables through optimization of the proposed model, an industrial example is adapted from [21]. A company with 125 working days per year sells a particular food product to a wholesaler in packages marked with a specific weight. Table 2 shows the nominal values of the parameters. Moreover, the number of simulation runs is set to 500 to compute the values of the average run length. The bounds of the constraints are assigned to limit the feasible space, as shown in Table 3.

Accordingly, the statistically acceptable lower and upper bounds are considered for  $ARL_0$  and  $ARL_1$ . The time interval for implementing the PM policy is limited by considering a lower bound of 5 hours. In addition, economic and statistical considerations necessitate setting limits on the decision variables. The maximum values of sample size, sampling interval, and the number of samplings are set in this regard. Since the required time to sample and plot each observation is about 0.01 hours,  $h$  is limited by the lower bound of 0.01. Generally,  $K$  is defined as one-half the size of the shift in terms of standard deviation [26]. Assuming  $\delta=2$ , it is reasonable to set  $k_c$  between 0.25 and 2.00. The smoothing parameter is not allowed to go beyond the defined interval. Besides,  $H$  is mainly defined as five times the standard deviation of an underlying process ( $h_c=5$ ). However, for autocorrelated processes in [15], there were cases with optimal values of about 42 for  $h_c$ . Thus, we bounded it between 1 and 80.

After implementing the codes written in MATLAB (R2016b) software, the optimal sets of decision variables are attained respectively for the MEC and ARMA charts as follows:

$$\{n, h, h_c, k, \lambda_c, k_c\} = \{1, 0.19, 8.34, 26, 0.809, 0.651\},$$

$$\{n, h, l, k, \theta, \phi\} = \{1, 0.23, 2.74, 22, 0.000, 0.617\}.$$

According to the results of the MEC chart, it is proposed to set the decision interval value at  $8.34\sigma_z$ . Moreover, a single sample should be



inspected every 0.19 hours, and after inspecting 26 samples consecutively, PM should be implemented. Table 4 shows the results of using both charts regarding cost, time, and production values. Focusing on the results of MEC, it is understood that the EPQ of 518 is optimally obtained with an expected total cost of 4944.79. Therefore, the total demand of 10000 can be produced after about 19.31 production cycles (10000 divided by 518).

On the other hand, a lower ETC value of 4934.12 is experienced using the ARMA chart [21]. Moreover, since its in-control time as  $T_{in}=5.11$  is

higher than  $T_{in}=5.06$  of using MEC, more quantity ( $Q$ ) is produced. The out-of-control time of the ARMA chart is also lower. The total demand of 10000 can be produced after 19.10 production cycles. It is lower than 19.31 production cycles obtained by MEC. In this particular case, it is suggested to use the ARMA monitoring technique because of earlier response to the demand with a lower expected total cost. In subsection 7.3, comprehensive comparisons are provided between two monitoring techniques to find the preferred one.

**Tab. 2. Values of the parameters in the numerical example**

Parameter	$\mu$	$\sigma_x^2$	u	v	$\delta$	$\lambda$	w
Value	100	10	0.475	0.01	2	0.01	1
Parameter	E	$T_1$	p	d	D	A	B
Value	0.01	1	100	80	10000	60	10
Parameter	$C_{in}$	$C_{out}$	$C_f$	$C_v$	$C_Y$	$C_{pm}$	$C_{rm}$
Value	115	950	1	0.2	200	2400	5000

**Tab. 3. Assigned values on the bounds of the constraints**

Bound	$ARL_0^{min}$	$n_{min}$	$n_{max}$	$h_{min}$	$h_{max}$	$h_{c min}$	$h_{c max}$
Value	200	1	20	0.01	6	1	80
Bound	$ARL_1^{max}$	$k_{min}$	$k_{max}$	$\lambda_{c min}$	$\lambda_{c max}$	$k_{c min}$	$k_{c max}$
Value	10	1	70	0.001	0.999	0.25	2.00
Bound	$R_{Int}$	$l_{min}$	$l_{max}$	$\theta_{min}$	$\theta_{max}$	$\phi_{min}$	$\phi_{max}$
Value	5	0.001	5	0.001	0.999	0.001	0.999

**Tab. 4. Comparison between the MEC and ARMA charts through cost, time, and production terms**

Control chart	E(Q)	E(S)	E(M)	E(I)	ETC	$T_{in}$	$T_{out}$	Q
MEC	692.86	31.10	2547.73	1673.10	4944.79	5.06	0.12	518.0
ARMA	690.63	26.28	2547.59	1669.63	4934.12	5.11	0.11	523.5

**7.2. Sensitivity analysis**

In this subsection, we investigate the effects of model parameters on the optimized solutions of the proposed model. The sensitivity analysis is performed using an orthogonal-array Taguchi design. The expected total cost is treated as a response variable, and thirteen independent variables are considered as factors. Table 5 shows the corresponding level plannings. Table 6 shows how independent variables are assigned to the trials of the  $L_{36}$  array. The optimized value of ETC for each trial is shown in the last column of Table 6.

The statistical software Minitab (version 18) is used to present analyses. The normality assumption of the ETC values is confirmed using the Anderson-Darling (AD) test with the  $p$ -value

of 0.522. Table 7 shows the Minitab output for the expected total cost per hour. A significance level of 0.05 is assumed. Thus, the factors  $w$ ,  $C_{in}$ , and  $C_{pm}$  are detected significant. Figure 3 shows the impacts of factor levels on the mean of ETC values. The lowest mean values of ETC are desired. Accordingly, when a larger shape parameter of the truncated Weibull distribution is considered, the value of ETC is expected to reduce. Moreover, the smaller values of the quality loss cost in the in-control state and the preventive maintenance cost lead to the decreased expected total cost.

Due to the significant effect of some input factors on the optimal ETC results, and that the estimation of those factors is more likely to fluctuate because of various internal and external

issues, the role of management in decision-making and attention to costs becomes more

noticeable.

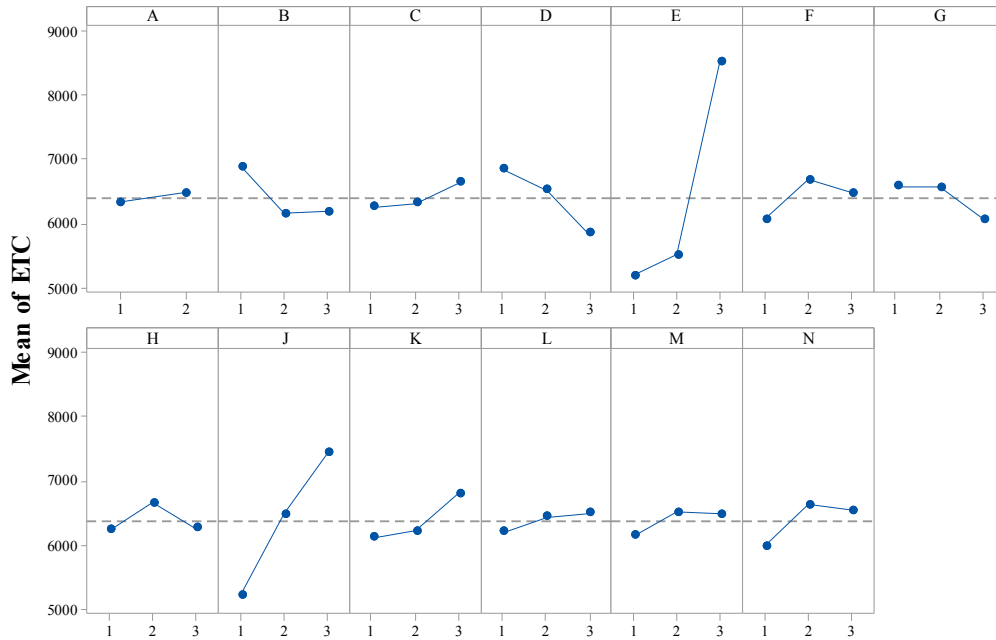


**Fig. 3. Main effects plot on the mean of ETC**

**Tab. 5. Level plannings of factors for the sensitivity analysis**

Factor Notation	A	B	C	D	E	F	G	H	J	K	L	M	N
	$\delta$	$u$	$\lambda$	$w$	$C_{in}$	$C_{out}$	$C_f$	$C_v$	$C_{pm}$	$C_{rm}$	$C_Y$	$E$	$T_1$
Level 1	1	0.00	0.01	0.5	50	100	0.5	0.2	1000	2500	50	0.01	0.1
Level 2	4	0.25	0.03	1.0	115	950	1.0	0.5	2400	5000	200	0.05	1.0
Level 3	-	0.75	0.05	2.0	700	1500	4.0	2.0	4000	7500	500	0.20	2.0

**Tab. 6. Levels of factors and optimization outputs for generated trials with the Taguchi L36 design**

Trial	Levels of factors														ETC
	A	B	C	D	E	F	G	H	J	K	L	M	N		
1	1	1	1	1	1	1	1	1	1	1	1	1	1	3315.3	
2	1	2	2	2	2	2	2	2	2	2	2	2	2	6258.0	
3	1	3	3	3	3	3	3	3	3	3	3	3	3	9307.8	
4	1	1	1	1	1	2	2	2	2	3	3	3	3	6361.8	
5	1	2	2	2	2	3	3	3	3	1	1	1	1	3667.2	
6	1	3	3	3	3	1	1	1	1	2	2	2	2	5565.3	
7	1	1	1	2	3	1	2	3	3	1	2	2	3	10660.0	
8	1	2	2	3	1	2	3	1	1	2	3	3	1	3447.2	
9	1	3	3	1	2	3	1	2	2	3	1	1	2	7686.6	
10	1	1	1	3	2	1	3	2	3	2	1	3	2	6597.1	
11	1	2	2	1	3	2	1	3	1	3	2	1	3	8844.7	
12	1	3	3	2	1	3	2	1	2	1	3	2	1	5736.8	
13	1	1	2	3	1	3	2	1	3	3	2	1	2	6184.7	
14	1	2	3	1	2	1	3	2	1	1	3	2	3	4043.6	
15	1	3	1	2	3	2	1	3	2	2	1	3	1	7608.3	
16	1	1	2	3	2	1	1	3	2	3	3	2	1	5184.4	
17	1	2	3	1	3	2	2	1	3	1	1	3	2	9923.8	
18	1	3	1	2	1	3	3	2	1	2	2	1	3	3335.9	
19	2	1	2	1	3	3	3	1	2	2	1	2	3	9153.0	
20	2	2	3	2	1	1	1	2	3	3	2	3	1	6797.8	
21	2	3	1	3	2	2	2	3	1	1	3	1	2	3801.6	

22	2	1	2	2	3	3	1	2	1	1	3	3	2	9205.0
23	2	2	3	3	1	1	2	3	2	2	1	1	3	4598.0
24	2	3	1	1	2	2	3	1	3	3	2	2	1	7214.4
25	2	1	3	2	1	2	3	3	1	3	1	2	2	5180.6
26	2	2	1	3	2	3	1	1	2	1	2	3	3	4710.6
27	2	3	2	1	3	1	2	2	3	2	3	1	1	9023.8
28	2	1	3	2	2	2	1	1	3	2	3	1	3	7249.6
29	2	2	1	3	3	3	2	2	1	3	1	2	1	6575.3
30	2	3	2	1	1	1	3	3	2	1	2	3	2	4458.1
31	2	1	3	3	3	2	3	2	2	1	2	1	1	8079.2
32	2	2	1	1	1	3	1	3	3	2	3	2	2	6636.8
33	2	3	2	2	2	1	2	1	1	3	1	3	3	4260.7
34	2	1	3	1	2	3	2	3	1	2	2	3	1	5283.4
35	2	2	1	2	3	1	3	1	2	3	3	1	2	8134.2
36	2	3	2	3	1	2	1	2	3	1	1	2	3	5998.3

Tab. 7. Minitab output for the expected total cost

Source	D.F.	Adj. SS	Adj. MS	F-value	P-value
Model*	3	101705895	33901965	24.85	0.000
D: $w$	1	5896252	5896252	4.32	0.046
E: $C_{in}$	1	66763702	66763702	48.94	0.000
J: $C_{pm}$	1	29045940	29045940	21.29	0.000
Residual	32	43652639	1364145		
Total	35	145358534			

\*  $ETC = 1847 - 496 D + 1668 E + 1100 J$

### 7.3. Comparing the control charts

In this subsection, extensive comparisons are provided between two monitoring techniques. Three sizes of shifts ( $\delta$ ) in the process mean are assumed to occur. For each assumed size of  $\delta$ , 16 trials are planned by considering various combinations of autocorrelation coefficients to include processes of types AR(1) when ( $u \neq 0, v = 0$ ), MA(1) when ( $u = 0, v \neq 0$ ), and ARMA(1,1) when ( $u \neq 0, v \neq 0$ ). The other data on the industrial example from Table 2 and Table 3 are also used here.

Table 8 shows the results of comparing the  $ETC$  values. Each trial was optimized two times, and then a solution with the lowest  $ETC$  value was selected. Assuming  $\delta = 1$  and AR(1) with ( $u = 0.5, v = 0$ ), the value of  $ETC$  is bolded for the ARMA chart since it is lower than that of the MEC chart. When  $\delta$  increases in this case,  $ETC$  decreases. However, it needs more investigations to analyze the trends.

We used Minitab 18 software to provide the graphical output in Figure 4. From the boxplots of  $ETC$  values for the ARMA chart: (1) the skewed distributions, and (2) the declining variability and central tendency are inferred by increasing  $\delta$ . Similar results are confirmed using the MEC chart. By comparing the boxplots of both charts, the mean value of the results for the ARMA chart is lower than it for MEC. Moreover, using the ARMA chart leads to lower variability

and more precision. From Figure 4(c) using the ARMA chart, although the top plot indicates increased results by growing  $u$ , the bottom plot shows this trend in the opposite direction by reducing  $v$ . Such findings are deduced to some extent from Figure 4(d) but with higher variability for the MEC chart. Generally, except for  $v = 0.25$ , the ARMA chart shows lower means of  $ETC$  values in the other cases.

From Table 8, it is observed that using the ARMA chart causes the lowest  $ETC$  in 32 cases. In comparison, MEC performs better in 18 cases. The weak performance of the MEC chart for larger shift sizes conforms to the concluding results in [15]. For more investigation, the paired  $t$ -test is used to determine whether the results of the two monitoring techniques differ [26]. The data in this test are paired to avoid differences among various levels of autocorrelation coefficients from disturbing the test on the difference between the control charts.

Before performing the test, the normality assumption must be confirmed. The top-left plot from Figure 5 shows the  $p$ -value of the AD test for the differences as (ARMA-MEC) is lower than 0.05. Accordingly, Johnson's transformation is applied to establish the normality assumption. After performing that, the assumption is statistically confirmed by achieving a  $p$ -value of 0.879. Therefore, the test can be executed on the transformed differenced data. Table 9 shows the

Minitab output for the paired  $t$ -test. From Table 9(c), the  $p$ -value of 0.614 suggests that the results are consistent with the null hypothesis. Indeed, the equal or better performance of the ARMA chart in comparison to the MEC chart can not be

rejected. This result can help the production manager to select the preferred monitoring technique for integrating the triple components in the presence of autocorrelation.

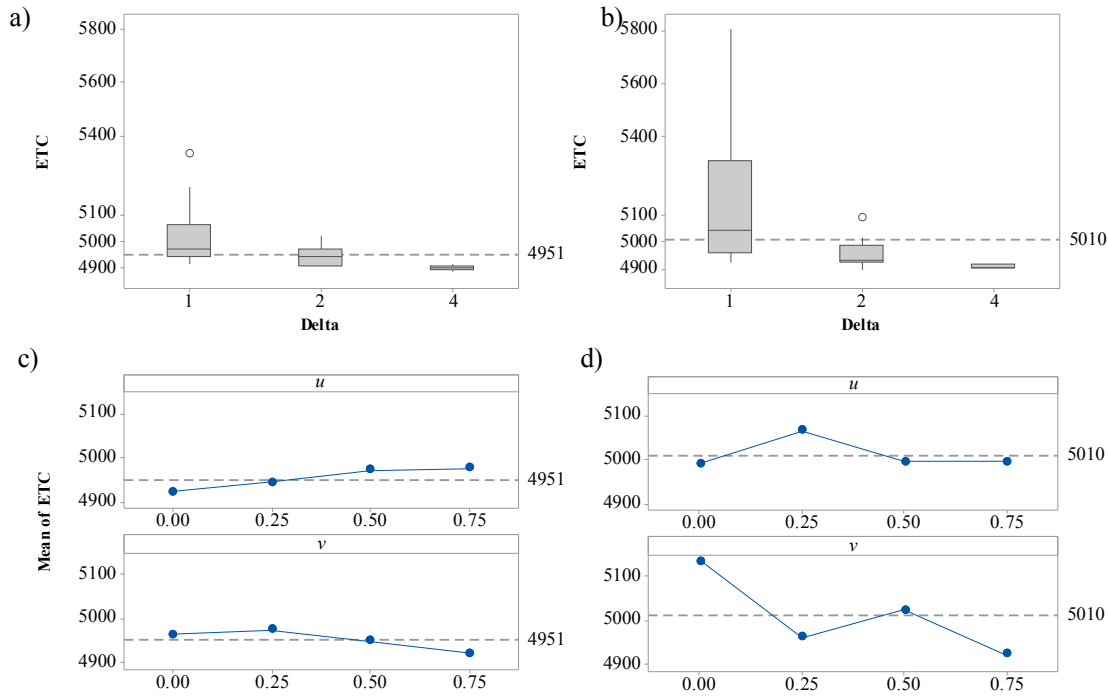


Fig. 4. Graphical output of Minitab: (a) boxplot of  $ETC$  using the ARMA chart v.s.  $\delta$ , (b) boxplot of  $ETC$  using the MEC chart v.s.  $\delta$ , (c) effects of autocorrelation coefficients on  $ETC$  using the ARMA chart, and (d) effects of autocorrelation coefficients on  $ETC$  using the MEC chart

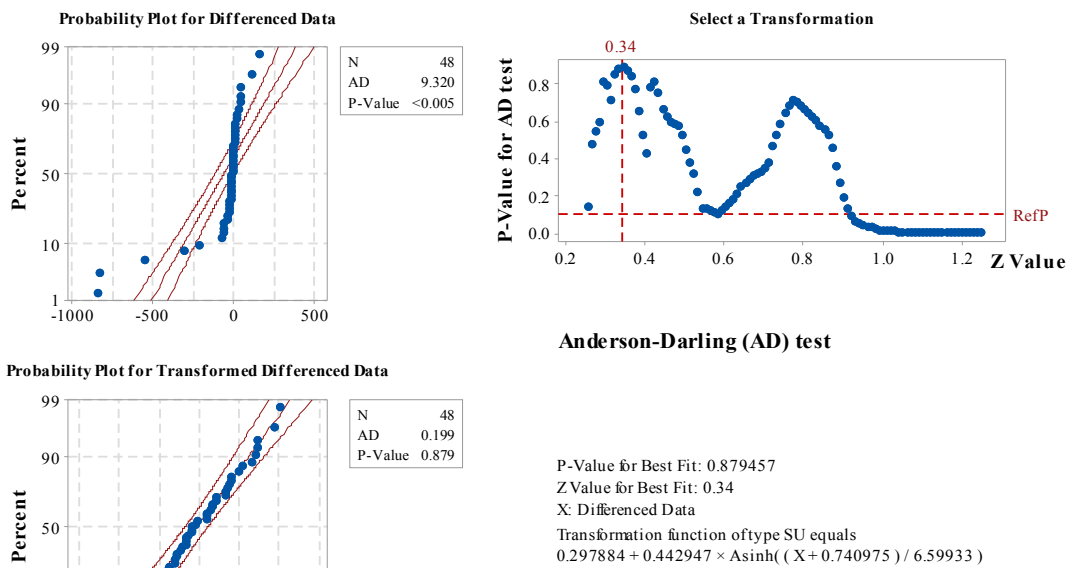


Fig. 5. Johnson transformation to establish the normal assumption for the differenced data

**Tab. 8. Comparing the ETC values of the ARMA and MEC charts by considering different autocorrelation coefficients**

Autocorrelation coefficients		$\delta=1$		$\delta=2$		$\delta=4$	
u	v	ARMA	MEC	ARMA	MEC	ARMA	MEC
0	0	4961	5805	4969	4928	4897	4897
	0.25	4943	4944	4906	4919	4884	4901
	0.5	4962	4975	4898	4897	4901	4895
	0.75	4940	4921	4897	4892	4880	4899
0.25	0	5172	5726	4939	4934	4904	4916
	0.25	5008	4963	4914	4928	4908	4901
	0.5	4969	5803	4909	4919	4892	4902
	0.75	4923	4925	4896	4936	4881	4917
0.5	0	5040	5346	4945	5010	4901	4911
	0.25	5326	5169	4952	4937	4897	4903
	0.5	4961	5028	4954	4946	4902	4902
	0.75	4934	4957	4901	4903	4909	4916
0.75	0	4912	5130	5017	5091	4890	4916
	0.25	5065	5057	4999	4998	4894	4917
	0.5	5203	5089	4934	4997	4890	4915
	0.75	5008	4976	4969	4926	4894	4896

**Tab. 9. Minitab output for the paired t-test**

(a) Descriptive statistics				
Sample	N	Mean	St. Dev.	S.E. Mean
ETC by ARMA	48	4951	87.4	12.6
ETC by MEC	48	5010	218.2	31.5
Difference	48	-58.9	193.5	27.9
(b) Test definition				
$\mu_{\text{difference}}$ : mean of (ETC by ARMA – ETC by MEC)				
Null hypothesis	$H_0: \mu_{\text{difference}} \leq 0$			
Alternative hypothesis	$H_1: \mu_{\text{difference}} > 0$			
(c) Test results				
Sample	Mean	St. Dev.	t-value	P-value
Transformed Difference	-0.043	1.009	-0.29	0.614

**7.4. Integrated design versus fixed-parameter designs**

A real data set, provided by Franco et al. [27], is used in this subsection for investigating the issue of separately setting some decision variables against the simultaneous determination of those variables. They examined the process of filling 125g yogurt containers and defined its weight as a variable qualitative characteristic. Due to the high production rate (approximately ten containers per second), inherent autocorrelation among the weights of successive productions has been confirmed. The previous studies have shown that the existing autocorrelation can be expressed with AR(1) by considering  $u=0.7$ . In addition, the mean and standard deviation

estimates were respectively estimated as 125g and 1g.

In monitoring this autocorrelated process, some recent samples have been detected out of control. The nozzle clogging of the filling machine has been introduced as the primary cause. The resulting non-conforming products and failed equipment can incur costs for the entire production system. On the other hand, yogurt production is based on responding to a demand. Therefore, it includes inventory holding and set-up costs in the framework of EPQ. Obviously, such a process requires: (1) implementing MP at the appropriate time to restore the process to the initial condition, (2) responding to the demand in quantity with the lowest production cost, and (3) using the descent SPC technique for monitoring

the AR(1) data. In fact, it seems necessary to study the integrated model in terms of autocorrelation due to the imperfectness of the production process and the presence of autocorrelation among the data.

Because of the equal or better performance of the ARMA chart in comparison to the MEC chart, we apply the ARMA chart in this subsection. The results of optimization for different fixed-parameter designs as well as the integrated design are presented in Table 10. Note that the fixed parameters were set according to [27], and the other decision variables were optimally determined. It is observed in Table 10 that the lowest ETC value is obtained for the integrated model, where all decision variables are simultaneously determined. It is worth mentioning that using the MEC for the integrated model results in  $ETC=4967.46$  with  $\{n, h, h_c, k, \lambda_c, k_c\}=\{1, 0.1, 9.25, 50, 0.771, 0.91\}$ .

In Table 11, 120 actual observations are presented to examine the statistical performance

of these designs. The ARMA control chart is used to depict different designs in Figure 6 according to the information from Table 10. The change point is assumed to occur in the 14<sup>th</sup> group sampling and the 66<sup>th</sup> individual sampling. Only in sections (c) and (d) of Figure 6, the ARMA chart can detect the change. For the design with a fixed sample size, this change is detected in the 20<sup>th</sup> sample. Since the time interval between samplings is 2.5 hours, it takes 15 hours to detect after the 14<sup>th</sup> sample. The same change, in the 98<sup>th</sup> sample with a time interval of 0.2 hours between samplings, is detected by the integrated design in 6.4 hours. Thus, the performance of the integrated design by simultaneous determination of the decision variables is confirmed in terms of economic and statistical criteria. In comparison to the designs that ignore simultaneous consideration of EPQ, SPC, and MP, it is suggested to optimize the integrated model of triple components because of its explicit benefits.

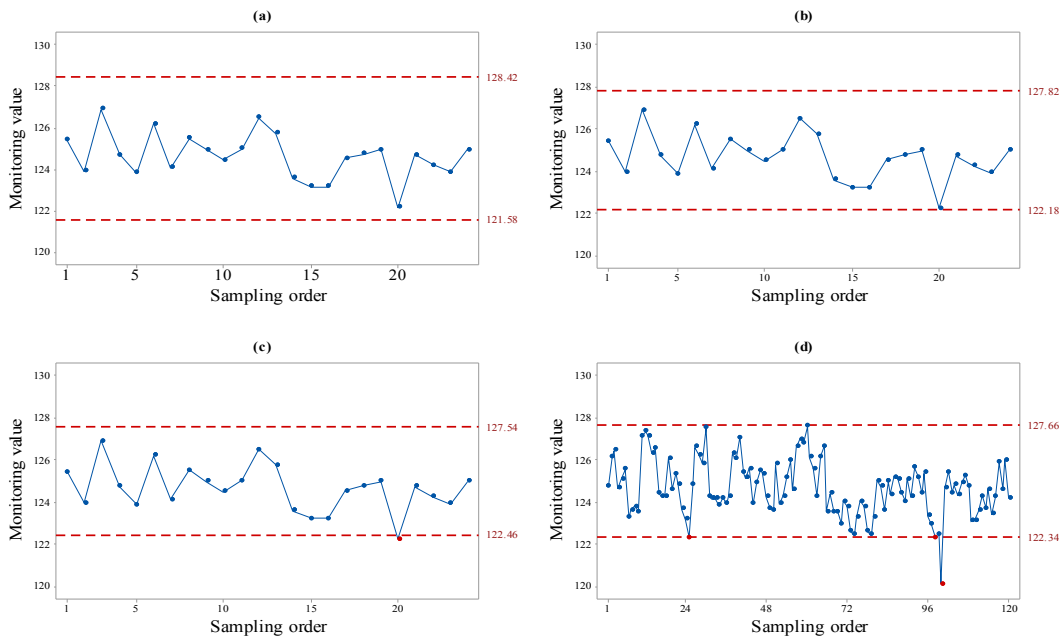


Fig. 6. The performance of different designs: (a) with fixed  $n, h, k$ , (b) with fixed  $n, h$ , (c) with fixed  $n$ , (d) with simultaneous determination of all variables

Tab. 10. Comparing the results of different designs using ARMA control chart

Design	$n$	$h$	$l$	$k$	$\theta$	$\phi$	ETC
Fixed ( $n, h, l$ )	5	1.00	3.00	5	0.14	0.60	5142.10
Fixed ( $n, h$ )	5	1.00	2.54	5	0.00	0.58	5114.74
Fixed ( $n$ )	5	2.50	2.48	2	0.00	0.68	5333.09
Integrated	1	0.20	2.55	25	0.00	0.66	4968.17

**Tab. 11. The yogurt container weight data set (read up to down, from the left side)**

124.74	127.18	125.37	124.22	125.40	125.79	126.15	124.02	125.03	124.22	124.65	123.59
126.12	127.38	124.87	124.15	125.14	123.91	125.60	123.78	124.72	125.64	125.45	124.27
126.45	127.18	123.65	124.14	125.60	124.28	124.26	122.60	123.62	125.19	124.43	123.70
124.66	126.32	123.16	123.82	123.90	125.19	126.17	122.42	124.99	124.39	124.83	124.62
125.11	126.55	122.29	124.18	124.92	125.98	126.65	123.26	124.37	125.40	124.34	123.41
125.56	124.41	124.83	123.91	125.53	124.55	123.54	124.02	125.17	123.35	124.88	124.24
123.24	124.22	126.62	124.28	125.36	126.61	124.42	123.78	125.10	122.90	125.27	125.87
123.60	124.29	126.24	126.31	124.24	126.98	123.52	122.60	124.45	122.31	124.73	124.62
123.77	126.10	125.86	126.06	123.71	126.84	123.53	122.42	124.03	122.42	123.09	125.99
123.54	124.60	127.53	127.08	123.64	127.60	122.95	123.26	125.11	120.09	123.14	124.19

**8. Conclusion**

Intending to consider real production conditions, we presented an integrated model in this study by incorporating three components of statistical process control, maintenance policy, and production. Control charts, among SPC tools, have mainly been developed to monitor process data under the assumption of independence. In some production processes, the assumption that the observations derived from the process are independent may not be valid. The existence of autocorrelation among the process data can result in a significant effect on the statistical performance of control charts if ignored. In literature, the ARMA control chart is a suitable technique for monitoring autocorrelated processes. By applying the ARMA chart, the integrated models had been studied in the presence of autocorrelation for the first time [21, 22].

Nevertheless, it was necessary to use another monitoring technique for comparing the results. Among the modified control charts, MEC had successfully been applied to monitor AR(1) process. However, it had not been studied for other types of autocorrelation, such as ARMA(1,1) and MA(1). In addition, only its statistical performance had been investigated. While designing MEC requires attention to the resulting costs as well. Attempting to bridge the mentioned gaps could be more realistic in the framework of the imperfect production systems. Thus, we presented an integrated model by considering the MEC monitoring technique. For optimizing the proposed model, the PSO algorithm was employed as a solution procedure. This procedure was applied through a numerical example. Then, sensitivity analysis was performed to identify the effects of model parameters on the optimal results. Moreover, some comparisons were made to compare the results of applying MEC and ARMA charts. Finally, a real data set was provided for investigating the issue of separately setting some

decision variables against the simultaneous determination of those variables.

In a particular case of an industrial example, it is suggested to use the ARMA monitoring technique because of the earlier response to the demand with a lower expected total cost. The results of comparative studies indicated that: (1) lower cost values are expected to reach by decreasing autoregressive coefficient and increasing moving average coefficient, (2) the results are less influenced by changing autocorrelation coefficients when the ARMA chart is used, and (3) except for  $\nu=0.25$ , ARMA chart shows lower cost values with smaller variability. Accordingly, the ARMA chart can be preferred, although the equal performance of both charts is not be rejected. The process of filling yogurt containers was also examined. It was found that the results of integrated design were better than designs that ignore simultaneous consideration of EPQ, SPC, and MP. In addition, the results of the sensitivity analysis confirmed that three factors, including the shape parameter of the truncated Weibull distribution, the quality loss cost in the in-control state, and the preventive maintenance cost, were significant. Due to the significant effect of some factors on the optimal ETC results and that the estimation of their values fluctuates because of various internal and external conditions, there is a need for designing models when such uncertainty exists in estimating factors. In [8, 9], robust optimization approaches have been proposed only by considering SPC in modeling under the assumption of independence. Therefore, the robust design of the integrated models can be pursued in the presence of autocorrelated data. Recently, among residual control charts, Chen and Yu [28] developed a control chart based on deep recurrent neural networks. In the category of modified control charts, an EWMA chart based on the likelihood-ratio test or ELR chart has been proposed to simultaneously monitor the shifts in mean and variability [29]. Moreover, Costa and Fichera [20] proposed the ARMA control chart

with variable sampling intervals. These control charts can be applied in similar models to provide guidelines in selecting the most compatible one(s). For high yield processes, two studies have been presented respectively in [30, 31]. Both can be extended for optimally selecting the decision variables by the integrated triple-component model. For the time being, we are trying to extend the ACC chart for autocorrelated processes.

### 9. Acknowledgments

The authors would like to acknowledge editors and reviewers of the paper for their important guiding and comments. This work was supported by the Iran National Science Foundation (INSF) [grant number 97015328].

### References

- [1] Cheng, L., Tsou, C.S., Yang, D.Y., "Cost-service tradeoff analysis of reorder-point-lot-size inventory models", *Journal of Manufacturing Systems*, Vol. 37, No. 1, (2015), pp. 217-226.
- [2] Salmasnia, A., Abdzadeh, B., Namdar, M., "A joint design of production run length, maintenance policy and control chart with multiple assignable causes", *Journal of Manufacturing Systems*, Vol. 42, (2017), pp. 44-56.
- [3] Salmasnia, A., Kaveie, M., Namdar, M., "An integrated production and maintenance planning model under VP-T2 Hotelling chart", *Computers & Industrial Engineering*, Vol. 118, (2018), pp. 89-103.
- [4] Salmasnia, A., Soltani, F., Heydari, E., Googoonani, S., "An integrated model for joint determination of production run length, adaptive control chart parameters and maintenance policy", *Journal of Industrial and Production Engineering*, Vol. 36, No. 6, (2019), pp. 401-417.
- [5] Hadidi, L.A., Al-Turki, U.M., Rahim, A., "Integrated models in production planning and scheduling, maintenance and quality: a review", *International Journal of Industrial and Systems Engineering*, Vol. 10, No. 1, (2012), pp. 21-50.
- [6] Farahani, A., Tohidi, H., "Integrated optimization of quality and maintenance: A literature review", *Computers & Industrial Engineering*, Vol. 151, (2021), p. 106924.
- [7] Qiu, P., "Some Recent Studies in Statistical Process Control", in Lio, Y., Ng, H. K.T., Tsai, T.-R., Chen, D.-G. (Eds.) *Statistical Quality Technologies: Theory and Practice*, Springer International Publishing, Cham, (2019), pp. 3-19.
- [8] Jafarian-Namin, S., Fallahnezhad, M.S., Tavakkoli-Moghaddam, R., Mirzabaghi, M., "Robust Economic-Statistical Design of Acceptance Control Chart", *Journal of Quality Engineering and Production Optimization*, Vol. 4, No. 1, (2019), pp. 55-72.
- [9] Jafarian-Namin, S., Fallahnezhad, M.S., Tavakkoli-Moghaddam, R., Mirzabaghi, M., "Robust modeling of acceptance control chart to specify best design parameters", in Shabazova, S.N., Kacprzyk J., Balas V., Kreinovich V. (Ed.) *Studies in Fuzziness and Soft Computing*, Springer Nature, Switzerland, (2021), pp. 321-332.
- [10] Mokhtari, H., Fallah Ghadi, H., Salmasnia, A., "Simultaneous optimization of production and quality in a deterioration process", *International Journal of Industrial Engineering and Production Research*, Vol. 27, No. 3, (2016), pp. 275-285.
- [11] Salmasnia, A., Abdzadeh, B., Rahimi, A., "Joint optimisation of double warning T2-Hotelling chart and maintenance policy with multiple assignable causes", *Journal of Statistical Computation and Simulation*, Vol. 90, No. 3, (2020), pp. 465-488.
- [12] Jafarian-Namin, S., Goli, A., Qolipour, M., Mostafaeipour, A., Golmohammadi, A.-M., "Forecasting the wind power generation using Box-Jenkins and hybrid artificial intelligence: A case study", *International Journal of Energy Sector*



- Management, Vol. 13, No. 4, (2019), pp. 1038-1062.
- [13] Alwan, L.C., Roberts, H.V., "The Problem of Misplaced Control Limits", *Journal of the Royal Statistical Society Series C*, Vol. 44, No. 3, (1995), pp. 269-278.
- [14] Thaga, K., Sivasamy, R., "Single Variables Control Charts: A Further Overview", *Indian Journal of Science and Technology*, Vol. 8, (2015), pp. 518-528.
- [15] Osei-Aning, R., Abbasi, S.A., Riaz, M., "Monitoring of serially correlated processes using residual control charts", *Scientia Iranica*, Vol. 24, No. 3, (2017), pp. 1603-1614.
- [16] Jiang, W., Tsui, K., Woodall, W.H., "A New SPC Monitoring Method: The ARMA Chart", *Technometrics*, Vol. 42, No. 4, (2000), pp. 399-410.
- [17] Low, C., Lin, W.Y., "Consideration of weibull distribution under the assignable causes for economic design of the ARMA control chart", *Journal of Quality*, Vol. 17, No. 5, (2010), pp. 365-387.
- [18] Lin, S.-N., Chou, C.-Y., Wang, S.-L., Liu, H.-R., "Economic design of autoregressive moving average control chart using genetic algorithms", *Expert Systems with Applications*, Vol. 39, No. 2, (2012), pp. 1793-1798.
- [19] Costa, A., Fichera, S., "Economic statistical design of ARMA control chart through a Modified Fitness-based Self-Adaptive Differential Evolution", *Computers & Industrial Engineering*, Vol. 105, (2017), pp. 174-189.
- [20] Costa, A., Fichera, S., "Economic-statistical design of adaptive arma control chart for autocorrelated data", *Journal of Statistical Computation and Simulation*, Vol. 91, No. 3, (2021), pp. 623-647.
- [21] Jafarian-Namin, S., Fallahnezhad, M.S., Tavakkoli-Moghaddam, R., Salmasnia A., Abooie, M.H., "An integrated model for optimal selection of quality, maintenance and production parameters with autocorrelated data", *Scientia Iranica*, (2021). DOI: 10.24200/sci.2021.56484.4745.
- [22] Jafarian-Namin, S., Fallahnezhad, M.S., Tavakkoli-Moghaddam, R., Salmasnia, A., Fatemi Ghomi, S.M.T., "An integrated quality, maintenance and production model based on the delayed monitoring under the ARMA control chart", *Journal of Statistical Computation and Simulation*, Vol. 91, No. 13, (2021), pp. 2645-2669.
- [23] Zhang, N.F., "A Statistical Control Chart for Stationary Process Data", *Technometrics*, Vol. 40, No. 1, (1998), pp. 24-38.
- [24] Niaki, S.T.A., Toosheghanian, M., Gazaneh, F.M., "Economic design of VSI  $\bar{X}$  control chart with correlated non-normal data under multiple assignable causes", *Journal of Statistical Computation and Simulation*, Vol. 83, No. 7, (2013), pp. 1279-1300.
- [25] Kennedy, J., Eberhart, R.C., *Swarm Intelligence*, Morgan Kaufmann, San Francisco, (2001).
- [26] Montgomery, D.C., *Introduction to statistical quality control*, Wiley, New Jersey, (2019).
- [27] Franco, B.C., Castagliola, P., Celano, G., Costa, A.F.B., "A new sampling strategy to reduce the effect of autocorrelation on a control chart", *Journal of Applied Statistics*, Vol. 41, No. 7, (2014), pp. 1408-1421.
- [28] Chen, S., Yu, J., "Deep recurrent neural network-based residual control chart for autocorrelated processes", *Quality and Reliability Engineering International*, Vol. 35, No. 8, (2019), pp. 2687-2708.
- [29] Wang, F.-K., Cheng, X.-B., "Exponentially weighted moving average chart with a likelihood ratio test for monitoring autocorrelated processes",

- Quality and Reliability Engineering International, Vol. 36, No. 2, (2020), pp. 753-764.
- [30] Fallahnezhad, M.S., Jafarian-Namin, S., Faraz, A., "Expanded fraction defective chart using cornish-fisher terms with adjusted control limits to improve in-control performance", International Journal of Industrial Engineering and Production Research, Vol. 30, No. 4, (2019), pp. 477-488.
- [31] Fallahnezhad, M.S., Golbafian, V., Rasay, H., Shamstabar, Y., "Economic-statistical design of a control chart for high yield processes when the inspection is imperfect", International Journal of Industrial Engineering and Production Research, Vol. 28, No. 3, (2017), pp. 241-249.

Follow This Article at The Following Site:

Jafarian-Namin S, Fallahnezhad M S, Tavakkoli-Moghaddam R, Salmasnia A, Abooei M H. A Comparative Study on a Triple-Concept Model of Two Techniques for Monitoring the Mean of Stationary Processes. IJIEPR. 2021; 32 (4) :1-18  
URL: <http://ijiepr.iust.ac.ir/article-1-1082-en.html>

